An Investigation of the Mixing Design and the Mechanical Properties of Glass and Date Palm Fibers and Nanoparticle-Polyester Hybrid Composites

Abousoufiane Ouis
Department of Mechanical Engineering, College of Engineering in Al-Kharj, Prince Sattam Bin Abdulaziz University, P.O. Box 655, Al-Kharj 16273, Saudi Arabia
a.ouis@psau.edu.sa (corresponding author)

Kamel Touileb
Department of Mechanical Engineering, College of Engineering in Al-Kharj, Prince Sattam Bin Abdulaziz University, P.O. Box 655, Al-Kharj 16273, Saudi Arabia
k.touileb@psau.edu.sa

Received: 19 May 2025 | Revised: 10 June 2025 | Accepted: 15 June 2025

Licensed under a CC-BY 4.0 license | Copyright (c) by the authors | *DOI: https://doi.org/10.48084/etasr.12241*

ABSTRACT

This study investigates, in the first stage, the mechanical properties of Glass Fiber (GF) and Date Palm Fiber (DPF)-reinforced polyester hybrid composites. Specimens were prepared with volume compositions of GF:DPF at 100:0%, 75:25%, 50:50%, 25:75%, and 0:100%. The results showed that the best Ultimate Tensile Strength (UTS) (23.00 MPa) was obtained for the 50:50% composition, while the highest absorbed energy (E-absor) in the impact test (3.76 J) was recorded for the 100:0% composition. In the second stage, the mechanical properties were further improved by incorporating nanoparticles: Carbon Nanotubes (CNT), Alumina (Al_2O_3), and Silica (SiO_2). A Design of Experiments (DOE) approach was carried out based on the best mechanical results, using ten nanoparticle-doped specimens. The mixing method in Minitab 17 software was used to identify the optimal combination, which was 88% CNT and 12% Al_2O_3. Consequently, the tensile strength increased to 35 MPa, and the (E-absor) reached 4 J.

Keywords-composites; GF; DPF; nanoparticles; mechanical properties; mixing design

I. INTRODUCTION

Sustainable materials are developed, utilized, and disposed of in ways that reduce the environmental impact and promote the social responsibility. They are typically renewable, recyclable, and biodegradable. Examples include natural fibers, such as palm fiber, cotton, hemp, and bamboo, as well as recycled resources, like plastics, glass, and metals. Among natural reinforcements, DPF have attracted growing interest due to their abundance, low cost, and biodegradability. In addition to DPF, various other natural fibers have been employed in composite materials, including sun hemp and Palmyra [1], kenaf (jute) [2], abaca [3], and silk fabric [4].

The Food and Agriculture Organization (FAO) has approved Saudi Arabia's proposal to designate 2027 as the International Year of the Date Palm. This initiative aims to highlight the crop's potential for sustainable cultivation under harsh climatic conditions and to support agribusiness systems that utilize its by-products. The date palm tree provides fruit, fiber, sheltering material, and fuel, making it a highly versatile and valuable resource. In parallel, the growing demand for lightweight, cost-effective, and sustainable materials has led to the development of hybrid composites, which incorporate more than one type of reinforcement. These materials offer superior mechanical performance compared to composites reinforced with a single fiber type. Many research studies have been conducted on DPF-matrix composites. Authors in [5] investigated the mechanical properties of palm fiber–polyester composites. Composite laminates (50% fiber and 50% matrix) were prepared using the hand lay-up method, and DPFs were collected from five different regions. Mechanical properties, such as tensile and impact strength, were evaluated. It was observed that the UTS of all samples increased compared to the neat matrix, except for one. The best tensile strength achieved was about 19.52% higher but still less than 15 MPa. The effect of the composition between sugar palm fiber (Arenga Pinnata) and polyester resin in composite materials was examined in [6]. The authors focused on the impact strength, tensile strength, and modulus of elasticity. Using mass fraction, the fiber-to-resin compositions were 30:70%, 40:60%, and 50:50%. The

50:50 ratio produced the highest values, with an average impact strength of $1.703*10^{16}$ kg/mm², tensile strength of 27.13 N/mm², and modulus of elasticity of 790.01 N/mm². DPF epoxy composites were fabricated with 40, 50, and 60 wt.% fiber loadings, and their tensile and impact properties were evaluated [7]. Increasing the DPF content up to 50% enhanced the mechanical strength and impact resistance compared to the neat epoxy resin.

Authors in [8] investigated the mechanical properties of DPF-reinforced phenolic composites at 0%, 40%, 50%, and 60 wt.% fiber loadings. The composites were manufactured using the hand lay-up technique and tested under tensile and impact loads. It was observed that incorporating 50% DPF improved the tensile modulus and impact properties but reduced the tensile strength. Hybrid composites with DPF have also been explored. Hybrid composites reinforced with DPF and GF in a vinyl ester matrix were studied [9]. The results showed that the GF reinforced samples had the highest tensile strength due to the superior mechanical properties of GF and its uniform fiber distribution.

The effect of combining palm fiber and GF with a polypropylene matrix was investigated in [10]. The inclusion of these fibers enhanced the tensile strength, thermal resistance, water resistance, and impact performance in the resulting composites. Mechanical properties, including the tensile strength, impact strength, and hardness, were analyzed in palm fiber/glass–epoxy woven laminate composites in [11], revealing multiple performance improvements. A biodegradable composite using Poly Lactic Acid (PLA) as matrix and untreated DPF fabric as reinforcement was fabricated in [12]. The results demonstrated strong adhesion between the fibers and matrix, which contributed significantly to the improved mechanical properties. Studies on polymer-based nanocomposites have highlighted the significant influence of nanoparticles on the mechanical and thermal behavior [13]. New polyethylene nanocomposites were developed using various processing methods and combinations of reinforcement types and contents [14, 15]. The results emphasized the impact of nanoparticles on the wear resistance, indentation resistance, creep behavior, and thermal stability. Hybrid composites were fabricated with 1 and 2 wt.% of Cellulose Nanofibers (CNF) via hand lay-up, followed by vacuum bagging and compression [16]. With 1 wt.% CNF, the tensile strength and modulus of GF–epoxy composites increased by 9% and 10%, respectively, while the flexural strength and modulus improved by 16% and 6%. The use of zirconium oxide (ZrO_2) nanoparticles in Unsaturated Polyester Resin (UPE) and E-glass composites was investigated in [17]. The addition of 2.5 wt.% ZrO_2 resulted in an impact resistance of 73.1 kJ/m², which significantly exceeded the value of 49.7 kJ/m² recorded for the commercial Chery bumper.

The microstructure and mechanical properties of carbon fiber–phenolic matrix composites were studied by incorporating CN and silicon carbide (SiC) nanoparticles [18]. The hybrid reinforcement strategy overcame the limitations of using each nanoparticle type individually. The combined addition enhanced the overall mechanical performance, with CN having a more pronounced effect per unit weight.

II. EXPERIMENTAL PROCEDURE

A. Mold Design and Fabrication

The mold parts were designed and fabricated with high-quality carbon steel sheets and assembled by laser welding. The mold, consisting of two female molds, allows the simultaneous production of two laminated samples and the mold covers are intended to obtain identical thicknesses for all samples, as shown in Figure 1.

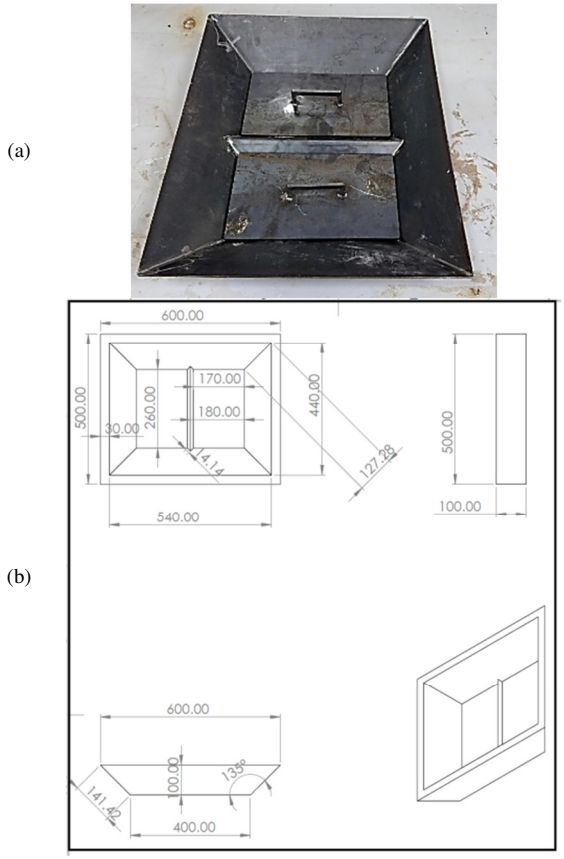

Fig. 1. (a) Closed mold for the laminates and (b) drawing of the mold (b). The dimensions are in mm.

B. Materials

The materials used included polyester resin as a matrix, hardener, honey wax as a release agent, sodium hydroxide (NaOH) powder for DPF cleaning, and acetone for general cleaning. The reinforcements consisted of GF in mat form, DPF, and nanopowders of CNT, Al_2O_3, and SiO_2. Sheets of GF mats were cut and DPF were prepared to fabricate 170×260×7 mm laminates, as depicted in Figure 2. Based on the density of GF ρ_{GF}=2.5 g/cm^3 and the density of DPF ρ_{DPF}=1.35 g/cm^3, and using a precision balance, mat sheets of GF and DPF were carried out. Figure 3 shows the laminates fabricated with different volume percentages according to Table I.

TABLE I. LAMINATES AND RELATED MASSES AND VOLUME PERCENTAGES

Sample #	Type	% Vol. GF	Mass GF (g)	% Vol. DPF	Mass DPF (g)
1	Neat resin	0	0	0	0
2	Pure GF	100	5.5×4=22	0	0
3	Hybrid composites	75	5.5×3=16.5	25	3.0×1=3
4		50	5.5×2=11	50	3.0×2=6
5		25	5.5×1=5.5	75	3.0×3=9
6	Pure DPF	0	0	100	3.0×4=12

Fig. 2. GF in mat form and prepared DPF (cleaned, dried, and shaped).

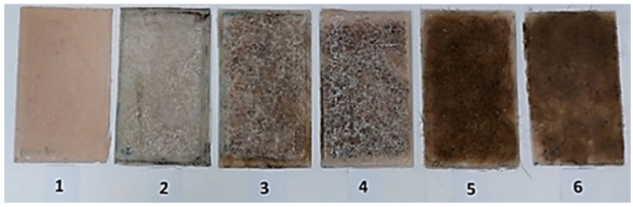

Fig. 3. Laminates extracted from the molds with GF:DPF volume ratios of: (1) neat resin, (2) 100:0%, (3) 75:25%, (4) 50:50%, (5) 25:75%, and (6) 0:100%.

The CNT, Al_2O_3, and SiO_2 nanoparticles, as displayed in Figure 4, used as reinforcing agents, were in powder form and characterized by diameters and lengths ranging from 10 to 30 nm, with a purity of 96% and a Specific Surface Area (SSA) of 150–200 mm²/g. Prior to their incorporation into the resin, the powders were individually preheated in a furnace at 80 °C for 2 h to remove moisture. A nanoparticle resin mixture was then prepared by dispersing 0.25 g of nanoparticles into 230 g of polyester resin using a mechanical stirrer operating at 900 rpm for 20 min at 60 °C. After mixing, the solution was allowed to cool for 10 min, followed by manual addition and mixing of the hardener.

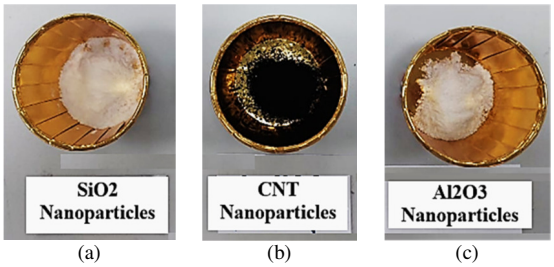

(a) (b) (c)

Fig. 4. (a) SiO_2 nanoparticles, (b) CNT nanoparticles, and (c) Al_2O_3 nanoparticles.

C. Mechanical Testing

Tensile tests were performed at room temperature using a computer-controlled electrohydraulic servo universal testing machine (model WAW-300E) at a crosshead speed of 0.5 mm/min, a loading rate of 0.5 kN/min, and a strain rate of 1.6×10^{-4} s^{-1}. The specimens were prepared according to ASTM D638-00 Type D. The measured mechanical property was the strength, expressed as UTS. Charpy impact tests were also conducted at room temperature using a JBS-500 impact test machine. Standard test procedures for plastics and composites were followed according to ASTM D5942-96. The mechanical property evaluated was the toughness, characterized by the E-absor during fracture. Drawings of the tensile and impact test specimens are portrayed in Figure 5.

(a)

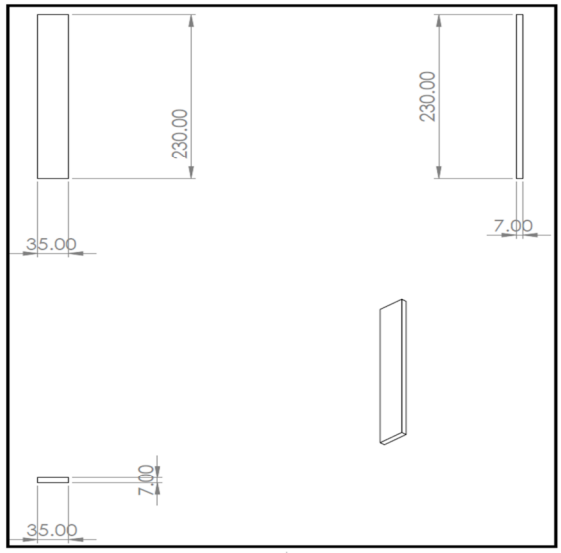

(b)

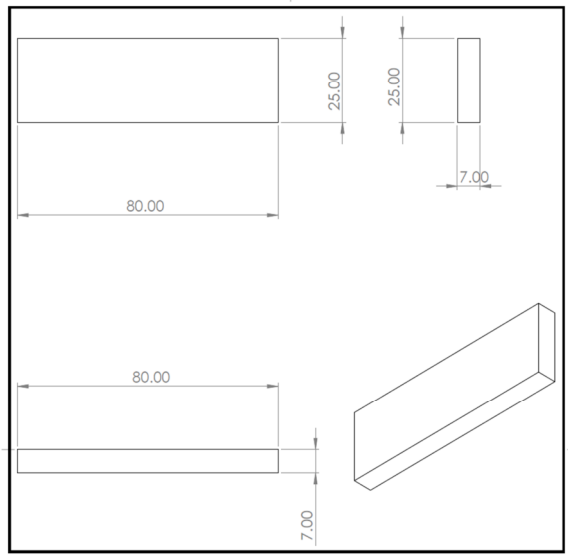

(b)

Fig. 5. (a) Tensile test specimen and (b) Charpy impact test specimen. The dimensions are in mm.

Figure 6 presents the fabricated tensile and impact test specimens reinforced with GF and DPF at various volume ratios, shown Figure 1(a) before, and Figure 1(b) after testing.

D. Design of Experiments

The mixing method in Minitab 17 was applied within the DOE framework to minimize the number of required experimental runs. This method is particularly proposed when combinations of two or more components are investigated simultaneously.

In this study, the centroid design of degree one, available in Minitab 17, was employed to generate ten mixing combinations from the three selected nanoparticles. The composition details are presented in Table II.

TABLE II. COMPOSITIONS OF NANOPARTICLES

Sample #	CNT	Al_2O_3	SiO_2
1	66.66	16.66	16.66
2	50	0	50
3	100	0	0
4	0	0	100
5	50	50	0
6	33.33	33.33	33.33
7	16.66	66.66	16.66
8	0	100	0
9	16.66	16.66	66.66
10	0	50	50

Figure 7 provides a schematic illustration of the fabrication steps of GF and DPF, and nanoparticle-polyester hybrid composites.

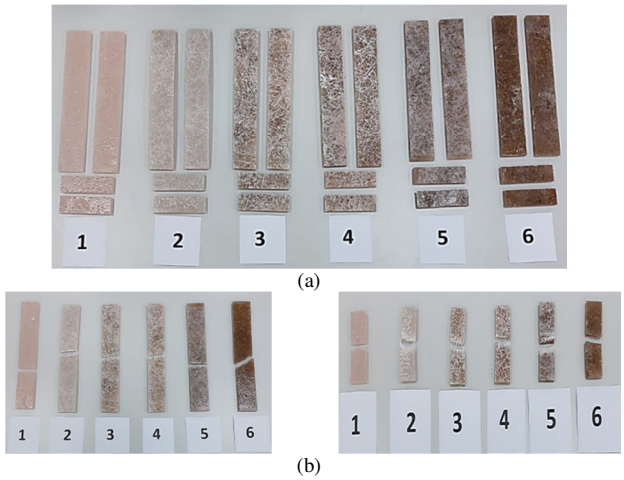

Fig. 6. Tensile and impact test specimens reinforced with GF and DPF at volume ratios GF:DPF of (1) neat resin, (2) 100:0%, (3) 75:25%, (4) 50:50%, (5) 25:75%, and (6) 0:100%: (a) before testing and (b) after testing.

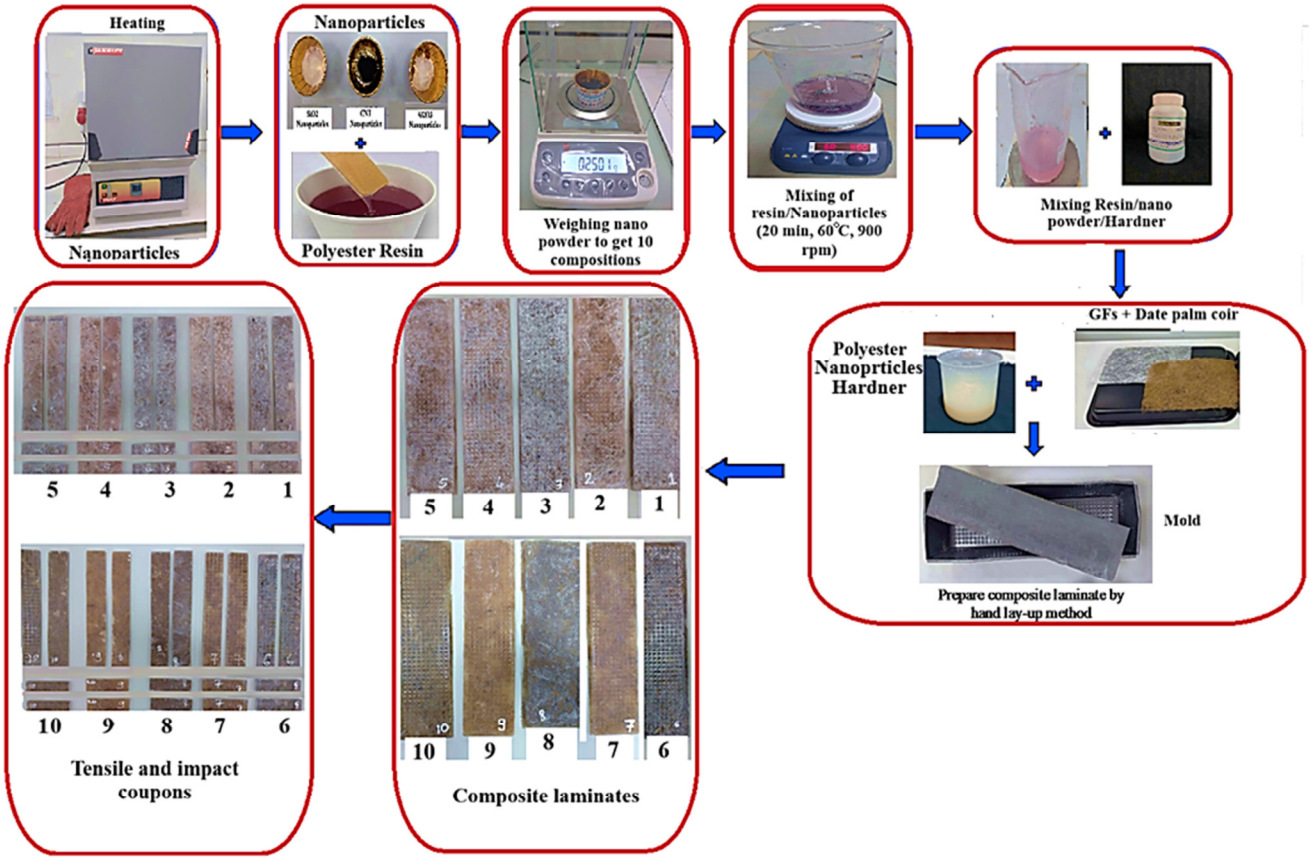

Fig. 7. Schematic illustration of fabrication of the GF and DPF, and nanoparticle-polyester hybrid laminate composites.

III. RESULTS AND DISCUSSION

A. Step 1: Tensile and Impact Tests

The tensile test of a sample containing 50% GF and 50% DPF exhibits the highest UTS up to 23 MPa, as displayed in Figure 8. Figure 9 shows that the maximum total E-absor, which is obtained for 100% GF (3.76 J), decreases almost linearly as a function of the DPF percentage. It reaches a value of (0.83 J) for 100% DPF.

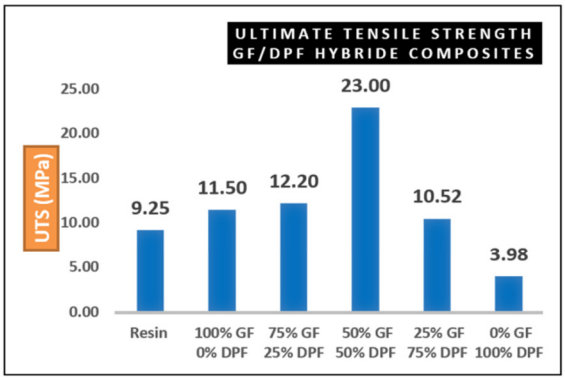

Fig. 8. Tensile test results of GF and DPF composites.

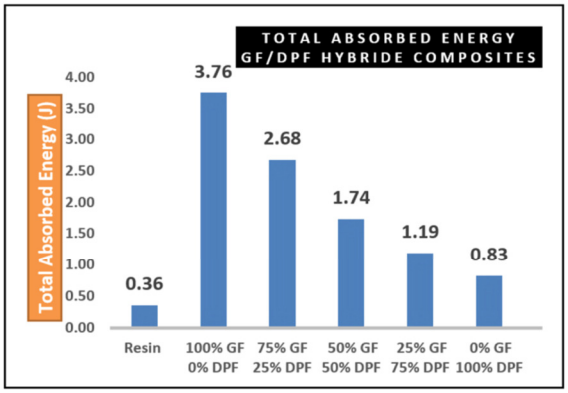

Fig. 9. Impact test results of the GF and DPF composites.

B. Step 2: DOE

Table III shows the UTS and E-absor results for different proportions (mixing combinations) of the three selected nanoparticles.

1) Regression Equation

In the present study, linear regression analysis was conducted using Minitab 17 software to develop predictive mathematical models for the dependent variables: UTS and E-absor, as functions of the nanoparticle content. No data transformation was applied to either response. The resulting predictive equations, obtained from the regression analysis, are:

$$UTS = 22.57 - 0.67CNT - 2.50Al_2O_3 \quad (1)$$

$$E - absor = 3.446 + 0.1367CNT - 0.1067Al_2O_3 \quad (2)$$

The validity of the developed regression models was evaluated using the coefficient of determination (R^2), which ranges from 0 to 1 (or 0% to 100% when expressed as a percentage). Higher R^2 values indicate a better fit between the dependent and independent variables. In the present study, the regression models for UTS and E-absor achieved high R^2 values of 96.16% and 99.71%, respectively.

Residual plots were used to assess the significance of the model coefficients. A linear pattern in the residual plot suggests that the residual errors are normally distributed, confirming the reliability of the model. The residual plots for UTS and E-absor are shown in Figure 10.

TABLE III. COMPOSITIONS OF NANOPARTICLES, STRENGTH, AND IMPACT ENERGY

#	Input variables			Output	
	CNT	Al_2O_3	SiO_2	Strength (MPa)	Impact energy (J)
1	66.66	16.66	16.66	21	3.74
2	50	0	50	17.5	3.48
3	100	0	0	21.5	3.85
4	0	0	100	26	3.74
5	50	50	0	21.5	3.62
6	33.33	33.33	33.33	18.5	3.5
7	16.66	66.66	16.66	11	3.23
8	0	100	0	17.5	3.25
9	16.66	16.66	66.66	20.5	3.35
10	0	50	50	19	3

(a)

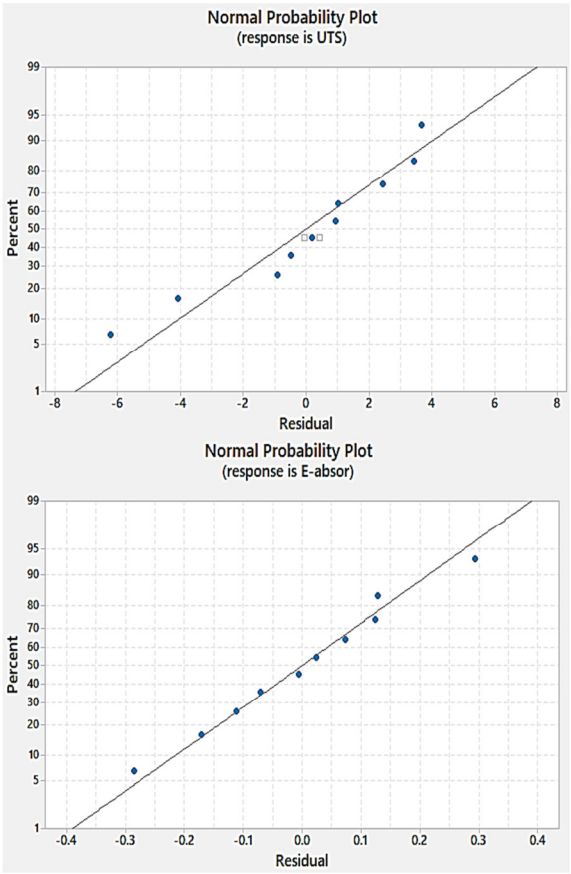

(b)

Fig. 10. Normal probability plots of the residuals for (a) UTS and (b) E-absor.

It was observed that the experimental results fall near the straight line for UTS and E-absor which implies that the developed model coefficients are significant.

2) Mixture Contour Plot

The mixture contour plots for UTS and E-absor, generated using Minitab 17, are presented in Figure 11. The iso-contour lines and the enclosed regions represent varying levels of tensile strength and impact energy. Different color gradients correspond to different property levels, with darker areas indicate the highest values. The analysis focuses on the regions where UTS and E-absor reach their maximum predicted values.

(a)

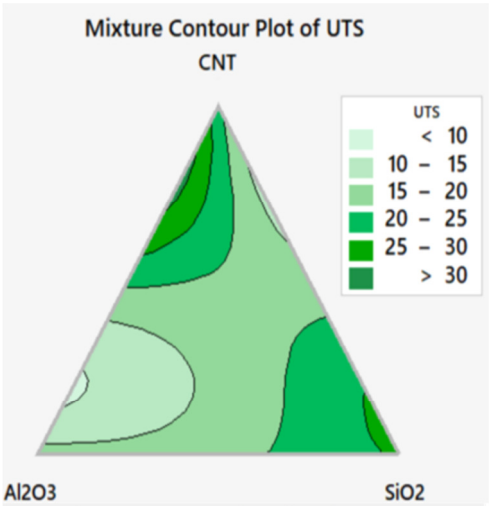

(b)

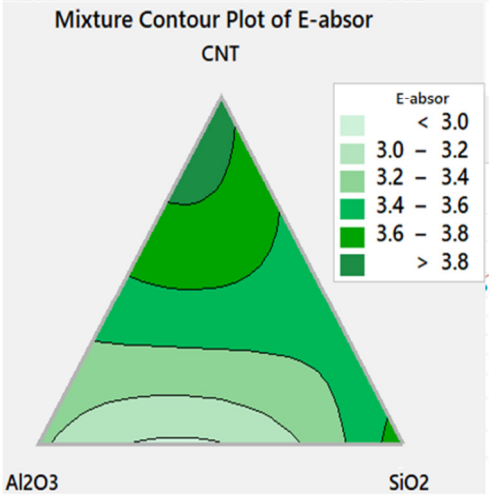

Fig. 11. Mixture contour plots for (a) UTS and (b) E-absor.

3) Optimization Plot

The optimization plot in Figure 12 shows how the three nanoparticle variables CNT, Al_2O_3, and SiO_2 influence the predicted values of UTS and E-absor. Each variable is plotted on a scale from 0 (lowest setting) to 3 (highest setting), while the middle point represents the optimal combination identified: 88% CNT, 12% Al_2O_3, and 0% SiO_2. This combination was obtained using the optimizer module available in Minitab 17.

In the left column of the plot, the predicted response for each property is shown along with a desirability score. For UTS, the predicted value is 30.17 MPa, with a desirability of 1.00, meaning that this result fully satisfies the optimization criteria. For E-absor, the predicted value is 3.80 J, with a desirability of 0.80. The overall desirability score for the composite is 0.90, indicating that the selected composition performs well for both target properties. These predicted values are summarized in Table IV and suggest that the fabricated composite is expected to exhibit mechanical behavior close to the optimal estimates.

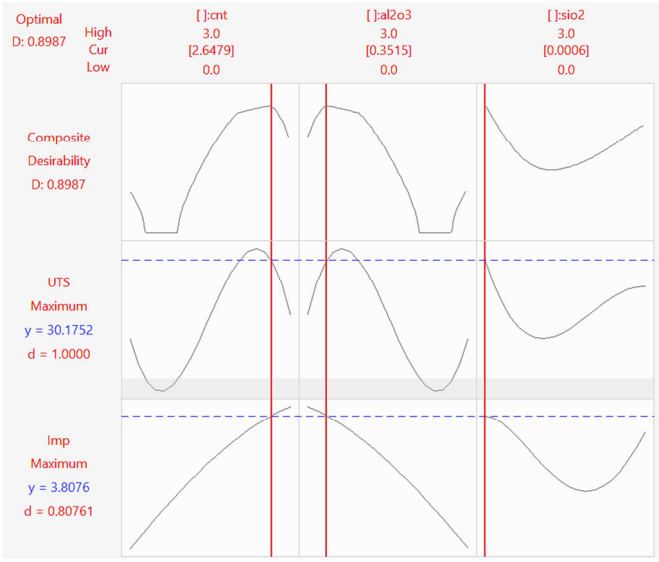

Fig. 12. Optimization plot for UTS and E-absor.

TABLE IV. PREDICTED RESPONSES OF THE COMPOSITE DOPED BY NANOPARTICLES

Responses	Predicted responses
UTS (MPa)	30.17
E-absor (J)	3.80

TABLE V. OPTIMALOPTIMAL COMPOSITION OF NANOPARTICLES

Variables	CNT	Al_2O_3	SiO_2
Percentages	88%	12%	0%

4) Experimental Validation

A composite was fabricated by the same technique. The sample was cut according to the abovementioned standards. The samples were tested in tensile and impact tests. The confirmation test is the last step in the experimental process. The experimental values of UTS and E-absor of the optimal combination are reported in Table VI. The results show that the UTS of the composite fabricated with the optimized composition is up to 35 MPa. The value obtained is greater than the value predicted by the software (30.17 MPa). Furthermore, the E-absor was enhanced to 4 J.

TABLE VI. STRENGTH AND E-ABSOR IN THE CASE OF OPTIMAL COMPOSITION

Responses	Experimental values
UTS (MPa)	35
E-absor (J)	4

IV. CONCLUSION

This study investigated the fabrication and mechanical characterization of hybrid composites reinforced with Glass Fiber (GF), Date Palm Fiber (DPF), and nanoparticles: Carbon Nanotubes (CNT), Alumina (Al_2O_3), and Silica (SiO_2) in a polyester matrix. The results demonstrated that both the fiber composition and the incorporation of nanoparticles significantly influenced the mechanical performance of the composites.

In the first stage, GF and DPF were combined at various volume ratios. The hybrid composite with a 50:50 GF:DPF ratio achieved the highest Ultimate Tensile Strength (UTS) of 23.00 MPa. The maximum absorbed energy (E-absor) in impact tests was recorded for the 100% GF composite (3.76 J), while the neat resin exhibited the lowest values for both UTS and E-absor. The impact of energy decreased almost linearly with increasing DPF content.

In the second stage, nanoparticles were introduced to the optimal 50:50 fiber configuration. Using a Design Of Experiments (DOE) approach with the mixing method in Minitab 17, ten different nanoparticle combinations were evaluated. The optimal formulation—88% CNT and 12% Al_2O_3—led to further enhancement of the mechanical properties, increasing UTS to 35 MPa and E-absor to 4 J.

These findings confirm that DPF is a viable sustainable reinforcement for polymer composites, and its combination with GF and selected nanoparticles can produce high-performance materials. Such hybrid composites, owing to their enhanced strength and impact resistance, hold promise for applications in various engineering sectors. Future research should focus on optimizing the nanoparticle selection and fiber–matrix interfacial bonding, particularly within biodegradable matrices, to advance the development of fully sustainable composite materials.

REFERENCES

[1] B. M. Dabade, G. R. Reddy, S. Rajesham, and C. U. Kiran, "Effect of Fiber Length and Fiber Weight Ratio on Tensile Properties of Sun hemp and Palmyra Fiber Reinforced Polyester Composites," *Journal of Reinforced Plastics and Composites*, vol. 25, no. 16, pp. 1733–1738, Nov. 2006, https://doi.org/10.1177/0731684406068418.

[2] M. S. Huda, L. T. Drzal, A. K. Mohanty, and M. Misra, "Effect of fiber surface-treatments on the properties of laminated biocomposites from poly(lactic acid) (PLA) and kenaf fibers," *Composites Science and Technology*, vol. 68, no. 2, pp. 424–432, Feb. 2008, https://doi.org/10.1016/j.compscitech.2007.06.022.

[3] A. Haneefa, P. Bindu, I. Aravind, and S. Thomas, "Studies on Tensile and Flexural Properties of Short Banana/Glass Hybrid Fiber Reinforced Polystyrene Composites," *Journal of Composite Materials*, vol. 42, no. 15, pp. 1471–1489, Aug. 2008, https://doi.org/10.1177/0021998308092194.

[4] S. P. Priya, H. V. Ramakrishna, S. K. Rai, and A. V. Rajulu, "Tensile, Flexural, and Chemical Resistance Properties of Waste Silk Fabric-reinforced Epoxy Laminates," *Journal of Reinforced Plastics and Composites*, vol. 24, no. 6, pp. 643–648, Apr. 2005, https://doi.org/10.1177/0731684405045024.

[5] S. Raghavendra and G. N. Lokesh, "Evaluation of mechanical properties in date palm fronds polymer composites," *AIP Conference Proceedings*, vol. 2057, no. 1, Jan. 2019, Art. no. 020021, https://doi.org/10.1063/1.5085592.

[6] A. K. Samlawi, P. R. Ansyah, and G. R. Cahyono, "Technical analysis of biocomposite reinforced with sugar palm (Arenga Pinnata) fiber for jukung materials," *IOP Conference Series: Materials Science and Engineering*, vol. 1034, no. 1, Oct. 2021, Art. no. 012154, https://doi.org/10.1088/1757-899X/1034/1/012154.

[7] N. Saba, O. Y. Alothman, Z. Almutairi, M. Jawaid, and W. Ghori, "Date palm reinforced epoxy composites: tensile, impact and morphological properties," *Journal of Materials Research and Technology*, vol. 8, no. 5, pp. 3959–3969, Sep. 2019, https://doi.org/10.1016/j.jmrt.2019.07.004.

[8] M. Asim, M. Jawaid, A. Khan, A. M. Asiri, and M. A. Malik, "Effects of Date Palm fibres loading on mechanical, and thermal properties of Date Palm reinforced phenolic composites," *Journal of Materials Research and Technology*, vol. 9, no. 3, pp. 3614–3621, May 2020, https://doi.org/10.1016/j.jmrt.2020.01.099.

[9] A. Merzoug, B. Bouhamida, Z. Sereir, A. Bezazi, A. Kilic, and Z. Candan, "Quasi-static and dynamic mechanical thermal performance of date palm/glass fiber hybrid composites," *Journal of Industrial Textiles*, vol. 51, no. 5, pp. 7599S-7621S, Jun. 2022, https://doi.org/10.1177/1528083720958036.

[10] S. Harish, D. P. Michael, B. Albert, M. L. Dhasan, and A. Rajadurai, "Mechanical property evaluation of natural fiber coir composite," *Materials Characterization*, vol. 60, pp. 44–49, Jan. 2009.

[11] K. Raju and M. Balakrishnan, "Evaluation of mechanical properties of palm fiber/glass fiber and epoxy combined hybrid composite laminates," *Materials Today: Proceedings*, vol. 21, pp. 52–55, Jan. 2020, https://doi.org/10.1016/j.matpr.2019.05.359.

[12] I. Ghanmi, F. Slimani, S. Ghanmi, and M. Guedri, "Development and Characterization of a PLA Biocomposite reinforced with Date Palm Fibers," *Engineering, Technology & Applied Science Research*, vol. 14, no. 2, pp. 13631–13636, Apr. 2024, https://doi.org/10.48084/etasr.6988.

[13] A. I. Gusev and A. A. Rempel, *Nanocrystalline Materials*, 1st ed. Cambridge, UK: Cambridge Int Science Publishing, 2004.

[14] A. S. Alghamdi, "Wear and Indentation Resistance of Polyethylene Nanocomposites at High Temperatures," *Engineering, Technology & Applied Science Research*, vol. 12, no. 4, pp. 9018–9022, Aug. 2022, https://doi.org/10.48084/etasr.4982.

[15] A. S. Alghamdi, "Synthesis and Mechanical Characterization of High Density Polyethylene/Graphene Nanocomposites," *Engineering, Technology & Applied Science Research*, vol. 8, no. 2, pp. 2814–2817, Apr. 2018, https://doi.org/10.48084/etasr.1961.

[16] T. Azhary, Kusmono, M. W. Wildan, and Herianto, "Mechanical, morphological, and thermal characteristics of epoxy/glass fiber/cellulose nanofiber hybrid composites," *Polymer Testing*, vol. 110, Jun. 2022, Art. no. 107560, https://doi.org/10.1016/j.polymertesting.2022.107560.

[17] N. M. Hayder and I. A. Mahmood, "Improving the Mechanical Properties of a Car Bumper by Using Glass Fiber Reinforced Composite Laminates and Nano-ceramic Filler," *Iraqi Journal of Industrial Research*, vol. 9, no. 2, pp. 100–108, Oct. 2022, https://doi.org/10.53523/ijoirVol9I2ID189.

[18] T. Subhani, "Microstructure and Mechanical Properties of Carbon Fiber Phenolic Matrix Composites containing Carbon Nanotubes and Silicon Carbide," *Engineering, Technology & Applied Science Research*, vol. 14, no. 2, pp. 13637–13642, Apr. 2024, https://doi.org/10.48084/etasr.7070.